Resilient Large-Scale Cognitive Radio Ad Hoc Networking Using Path-Time Codes

Yi-Chi Chen[1], I-Wei Lai[2] and Kwang-Cheng Chen[3]
Graduate Institute of Communication Engineering, National Taiwan University, Taiwan[1]
Department of Electrical Engineering, National Taiwan Normal University, Taiwan[2]
Department of Electrical Engineering, University of South Florida, USA[3]
E-mails: d03942009@ntu.edu.tw, iweilai0924@gmail.com, and kwangcheng@usf.edu

***Abstract*—Cognitive radio ad hoc networks (CRAHNs) emerge as a spectrum efficient networking technology to enable autonomous machine-to-machine communication among massive number of IoT devices. However, spectrum sharing results in opportunistic links and CRAHN becomes a kind of opportunistic networks. To reduce latency in CRAHN and to achieve overall spectrum efficiency by avoiding tremendous feedback signaling, CRAHNs of open-loop physical layer transmission open a new avenue under massive operations. The new technology challenge associated with such new CRAHNs lies in error control with only local networking information without relying on feedback control over each opportunistic link. Path-time codes virtually realizing multi-input-multi-output over network layer have been innovated to resolve such a dilemma. However, effective multipath routing considering interference remains unclear. In this paper, be taking network topological factors and interference into account, we analytically derive SINR approximations to design power control and multi-path greedy routing. By stochastic geometry analysis, we also show that the resilient operation for large-scale CRAHNs can be facilitated with the aid of path-time codes.**

Index Terms— Internet of things (IoT), machine-to-machine communication, cognitive radio ad hoc networks (CRAHNs), virtual multiple-input multiple-output (MIMO), space-time code, path-time code (PTC), stochastic geometry, Poisson point process (PPP).

I. Introduction

In cognitive radio ad hoc networks (CRAHNs), secondary users (SUs) are considered as unlicensed users with lower priority for channel access, while primary users (PUs) have highest priority for their licensed band. By utilizing dynamic spectrum sensing to access spectrum holes, a large amount of SUs devices are allowed to be co-existed with PUs, which greatly enhances the spectrum efficiency. Through many technological issues for CRAHNs, *e.g,* self-organization in resilient heterogeneous networks [1], efficient CRAHNs can easily support many application scenarios for Internet of Things (IoT). As the links in CRAHNs are opportunistic due to spectrum opportunities, the relay paths of end-to-end transmission can be vulnerable and unidirectional [2]. Furthermore, since only local information among SUs in the close vicinity is available, the centralized control requires tremendous control signaling that consumes good bandwidth. Instead of the conventional ad hoc networking of closed-loop communications that require tremendous overhead for the end-to-end information exchange and network control, the open-loop communication attracts attention to reduce latency and signaling bandwidth consumption [3], [4]. However, the resilient operation of CRAHNs can be a great challenge.

To resolve this technology dilemma, virtually utilizing multiple-input multiple-output (MIMO) and exploiting multiple transmission paths has been innovated to facilitate the error control of CRAHNs of open-loop communications [5], [6]. Novelly applied the well-investigated space-time codes (STC) of physical-layer MIMO systems, path-time codes (PTC) enhances the end-to-end transmission reliability by encoding the data along the time and path coordinate, on top of network layer. While previous virtual efforts [5], [6] focus on the code design given multipath routing, in this paper, we investigate the multipath routing for the PTC, particularly incorporating interference by concurrent transmissions in CRAHNs. Following the stochastic geometry to analyze interference, the PUs and SUs are randomly distributed according to the homogeneous Poisson point process (PPP) [7], [8]. The routing for multihop single-path has been well designed in the PPP network topology [9], [10] and further theoretical efforts, such as outage probability, transport capacity, and delay characterization in (single-path) multihop network [11], [12], have been investigated. On top of these fruitful results, we can comprehend the resilient network operation and the performance of CRAHN using PTCs with multipath routing and power control, under local networking information and without replying on feedback control signaling to improve latency.

In this paper, while error control to ensure resilient network operations, we optimize the mean number of hops that represents latency of networking. The near optimal routing policy is designed with respect to the network environment, *e.g.*, node density, interference level, and number of paths. Based on the *progress rule* [10] that maximizes the effective hop distance so as to minimize the number of hops for the path search, we propose a multipath-search algorithm for multipath routing and coding-aided scheme with PTC for error-resilient control and efficient end-to-end transmission in CRAHNs. With network topological factors and stochastic geometry analysis, we show that the resilient operation for large-scale CRAHNs can be facilitated with the aid of PTC.

This paper is organized as follows: In Section II, we introduce the virtual MIMO PTC end-to-end transmission. In Section III, we revisit stochastic geometry for PPP network and extend *progress rule* to propose a multipath-search algo-

978-1-4673-8999-0/17/$31.00 ©2017 IEEE

rithm for selecting relays as PTC transmission. In Section IV, based on the per-hop and end-to-end outage probability, the theoretical results focusing on per-hop transmit SNR on multiple paths are analyzed. Numerical simulations are presented in Section V, addressing the relation among reliability, power control, maximum allowance for waiting period, and number of hops under different interference levels. Finally, Section VI presents our main conclusions.

II. System model

Let the term *link* (or hop) denote the connection between two nodes, and *path* the end-to-end route between a pair of source ($\mathcal{S}$) and destination ($\mathcal{D}$) nodes. This work focuses on the case of distributed networking without centralized control. We consider multihop networking with K link-disjoint paths comprising $N_k - 1$ relay nodes, $k \in \{1, \ldots, K\}$. Such multihop/multipath routing can be established using the algorithms proposed in [13]–[15].

In this paper, we focus on developing a practical way for the multipath construction and investigate the influence caused from imperfect routes in PPP networks. Fig. 1 shows the $K = 3$ case without failed path in Fig. 1 (a) and with one-failed path due to interferers (PU transmitter) in Fig. 1 (b).

For the PTC transmission, defining χ as the constellation set, the source node encodes a data packet $\mathbf{x} \in \chi^M$ by a coding matrix $\tilde{\mathbf{C}} \in \mathbb{C}^{K \times M}$ and transmits the resulting coded packet at time instant m. Then, the equivalent received coded packet can be expressed as

$$\begin{aligned} y_m &= (\mathbf{h}_m \circ \mathbf{v}_m)^\top \tilde{\mathbf{C}}_m \mathbf{x} + \sum_{k=1}^{K} \tilde{\eta}_{m,k} \\ &= (\mathbf{h}_m \circ \mathbf{v}_m)^\top \tilde{\mathbf{C}}_m \mathbf{x} + \eta_m, \end{aligned} \tag{1}$$

where $(\cdot)^\top$ denotes transposition, $\tilde{\eta}_{m,k}$ is the noise aggregated from all links in the kth path, $\circ$ is the Schur product, $\mathbf{h}_m = [h_{m,1}, \ldots, h_{m,K}]^\top \in \mathbb{C}^K$ is the path fading gain, and $\mathbf{v}_m = [v_{m,1}, \ldots, v_{m,K}]^\top \in \{0,1\}^K$ to indicate if the coded packet is successfully propagated to the destination in the mth time instant through the kth path. The value of $h_{m,k}$ and $v_{m,k}$ are determined by the location of the selected relays, following a procedure described in Section III.

The received PTC-coded packets $\mathbf{y} = [y_1, \ldots, y_M]^\top \in \mathbb{C}^M$ from $m = 1$ to $m = M$ can be represented as

$$\begin{aligned} \mathbf{y} &= \begin{bmatrix} (\mathbf{h}_1 \circ \mathbf{v}_1)^\top & \ldots & \mathbf{0}^\top \\ \vdots & \ddots & \vdots \\ \mathbf{0}^\top & \ldots & (\mathbf{h}_M \circ \mathbf{v}_M)^\top \end{bmatrix} \underbrace{\begin{bmatrix} \tilde{\mathbf{C}}_1 \\ \vdots \\ \tilde{\mathbf{C}}_M \end{bmatrix}}_{\mathbf{C}} \mathbf{x} \\ &+ \underbrace{\begin{bmatrix} \eta_1 \\ \vdots \\ \eta_M \end{bmatrix}}_{\boldsymbol{\eta}} = \underbrace{\begin{bmatrix} (\mathbf{h}_1 \circ \mathbf{v}_1)^\top \tilde{\mathbf{C}}_1 \\ \vdots \\ (\mathbf{h}_M \circ \mathbf{v}_M)^\top \tilde{\mathbf{C}}_M \end{bmatrix}}_{\mathbf{H}_{\text{eq}}(\mathbf{V},\mathbf{C})} \mathbf{x} + \boldsymbol{\eta} \\ &= \mathbf{H}_{\text{eq}}(\mathbf{V}, \mathbf{C}) \mathbf{x} + \boldsymbol{\eta}, \end{aligned} \tag{2}$$

where the coding matrix $\mathbf{C} = [\tilde{\mathbf{C}}_1^\top, \ldots \tilde{\mathbf{C}}_M^\top]^\top \in \mathbb{C}^{KM \times M}$ represented cascaded $\tilde{\mathbf{C}}_m^\top$, and erasure indicator matrix $\mathbf{V} = [\mathbf{v}_1, \ldots, \mathbf{v}_M] \in \{1, 0\}^{K \times M}$. With the equivalent channel $\mathbf{H}_{\text{eq}}(\mathbf{V}, \mathbf{C})$, the formulation in (2) can be interpreted as virtual MIMO system where multiple nodes are coordinated to form the multihop/multipath route between the source and destination pair.

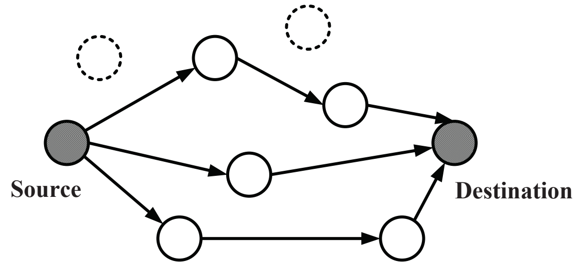

(a) Example of perfect routes, fully supported from selected relays, in the SU network without interference.

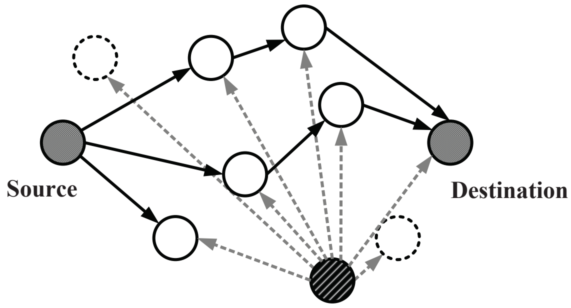

(b) Example of imperfect routes with one failed path caused from a PU transmitter as an interferer coexisted in the SU network.

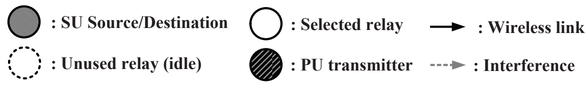

Fig. 1. Example topology of end-to-end transmission in a cognitive radio ad hoc networks (with multipath $K = 3$).

The PTC exploits path and time diversity to increase system reliability. In this paper, we adopt the discrete Fourier transform (DFT)-based PTC [6] where the (l, m)th entry of the coding matrix $\mathbf{C}$ takes the form of

$$C_{l,m} = \frac{1}{\sqrt{K}} e^{\frac{-j2\pi lm}{KM}}, \quad l = 1, \ldots, KM, \quad m = 1, \ldots, M. \tag{3}$$

This choice of the DFT-based PTC matrix $\mathbf{C}$ disperses $\mathbf{x}_m$ through all the K paths and M time instants. As long as $\mathbf{v}_m \neq \mathbf{0}$, all entries of the kth row vector of $\mathbf{H}_{\text{eq}}(\mathbf{V}, \mathbf{C})$ are nonzero. Thus, $\mathbf{x}$ is successfully received at time instant m, which results in increased diversity [6].

III. Random network topology via stochastic geometry

In Section II, the system model of PTC end-to-end transmission (2) is based on the assumption of perfect routing. In this paper, we propose a routing algorithm in the random network with local information. In random network, the failed path possibly occurs when no relay nodes are in the close vicinity, or signals are contaminated by severe interference.

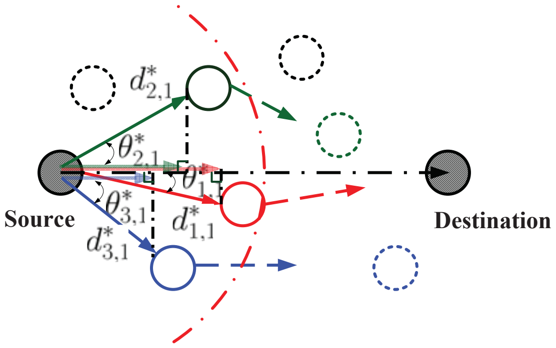

Fig. 2. Example to the multipath-search among SUs in (5) for no interference case: The red-dash-dotted curve (boundary) indicates the relay nodes are possibly selected for the maximum progress from $\mathcal{S}$ toward destination. With the selected relay $\{\mathcal{Z}_{k,n}\}$ corresponding to the nth hop in the kth path, $d^*_{k,n}$ and $\theta^*_{k,n}$ simply denoted for the effective hop distance $d\left(\mathcal{Z}_{k,n}\right)$ and angle $\theta\left(\mathcal{Z}_{k,n}\right)$. Notice that the 1st path-search (red-line) node can not support the 2nd path relaying. Thus, the 2nd path-search (green-line) selects another relay node with maximum progress value except occupied nodes and so on for the 3rd path (blue-line).

We leverage homogeneous Poisson point process (PPP) from stochastic geometry to simulate network topology. Since all $\mathcal{S}$–$\mathcal{D}$ pairs are stochastically equivalent, we investigate the performance at a typical $\mathcal{S}$–$\mathcal{D}$ pair [11] and consider SU network with randomly scattered relay nodes for PTC end-to-end transmission. We assume the $\mathcal{S}$–$\mathcal{D}$ pair is predetermined in a fixed distance, *i.e.,* $d_{\mathcal{S}-\mathcal{D}}$ is fixed. Let the locations of SUs be Φ_{SU} that follows homogeneous PPP with density λ_{SU}. For SUs co-existed with PUs, we consider SU network with interference caused from PU transmitters Φ_{PT} which also follow homogeneous PPP with density λ_{PT}. Thus, by the stationary of homogeneous PPP, the signal-to-interference-plus-noise ratio (SINR) requirement of a successful transmission for the nth link in the kth relay path can be represented as

$$\frac{P_{SU}G_{SU}|d(\mathcal{Z}_{k,n})|^{-\alpha}}{N_0+I_{PT}} \geq \beta, \tag{4}$$

where $I_{PT} = \sum_{\mathcal{I}_j\in\Phi_{PT}} G_{PT}P_{PT}|d_{\mathrm{E}}(\mathcal{I}_j,\mathcal{Z}_{k,n})|^{-\alpha}$ is the interference from PU transmitters $\{\mathcal{I}_j\}$ to the selected nodes located in the $\{\mathcal{Z}_{k,n}\}$, $d_{\mathrm{E}}(\cdot,\cdot)$ is the Euclidean distance, and $d(\mathcal{Z}_{k,n})$ is the nth hop distance in the kth relay path, *i.e.,* $d(\mathcal{Z}_{k,n}) = d_{\mathrm{E}}(\mathcal{Z}_{k,n-1},\mathcal{Z}_{k,n})$, $\mathcal{Z}_{k,0} = \mathcal{S}$ for all k, α is the path loss exponent, G_{SU}, G_{PT} are exponential distributed powers with unit mean, and β denotes the SINR requirement for successful transmission per-hop.

The *progress rule* indicates that maximizing the effective hop distance equals the minimization of the number of hops in a line [10]. We extend this path-search procedure from single-path to multipath. The selected relay — the nth hop in the kth path — could be generally expressed as

$$\mathcal{Z}^\star_{k,n} = \underset{\mathcal{D},\mathcal{Z}_{k,n}\in\Phi'_{SU}}{\arg\max}\ |d(\mathcal{Z}_{k,n})|\cdot\Big(\cos\big(\theta\{d(\mathcal{Z}_{k,n})\}\big)\Big)^+,$$
$$\text{s.t.}\quad \frac{P_{SU}G_{SU}|d(\mathcal{Z}_{k,n})|^{-\alpha}}{N_0+I_{PT}} \geq \beta,\ \text{from (4)}, \tag{5}$$

where Φ'_{SU} denotes Φ_{SU} excluding selected relay nodes, and $\theta\{\cdot\}$ is the operator for finding the angle between direction of potential relay and destination. Fig. 2 provides an example for the multipath-search procedure. The proposed multipath-search algorithm shows as follows:

Algorithm: Multipath-search algorithm

Initialize: Coded packet is transmitted from source node $\{S\} = \{\mathcal{Z}_{k,n} \mid k = 1,\ldots,K;\ n = 0\}$ with $\Phi'_{SU} = \Phi_{SU}$.
for $k = 1,\ldots,K$ *(as the kth path)* **do**
  Reset $n = 0$ for coded packet starting at $\{\mathcal{S}\}$;
  for $n = n+1$ *(as the nth hop)* **do**
    Calculate (5) and select $\{\mathcal{Z}^\star_{k,n}\}$;
    if $\{\mathcal{Z}^\star_{k,n}\} = \{\mathcal{D}\}$ *reaching destination* **then**
      Hop to $\{\mathcal{Z}^\star_{k,n}\}$ for constructed path;
    else
      if $\{\mathcal{Z}^\star_{k,n}\} \in \Phi'_{SU}$ **then**
        Hop to $\{\mathcal{Z}^\star_{k,n}\}$;
        Update $\Phi'_{SU} \leftarrow \Phi'_{SU}\backslash\{\mathcal{Z}^\star_{k,n}\}$;
      else
        For failed path;
      end
    end
  end
  Set $n = N_k$ hops in the kth path;
end
Find out all selected relays $\{\mathcal{Z}^\star_{k,n}\}$, $k = 1,\ldots,K$, $n = 1,\ldots,N_k$, supporting PTC-aided multipath routing.

For observing reception timing of the mth PTC coded packet at the destination, the per-hop fading gain $g_{m,k,n}[t]$ should satisfy SINR requirement in (4) with substitution $G_{SU} = |g_{m,k,n}[t]|^2$ for forwarding coded packets. The synchronized timing $t = T_{m,k,n} \in \mathbb{N}$ can be viewed as transmission trials (as random variables). For the mth coded packet transmitted in the kth path with N_k hops reaching destination, the total number of attempts can be expressed as $T_{m,k} = \sum_{n=1}^{N_k} T_{m,k,n}$, where $T_{m,k} \in \mathbb{N}$ for the mth coded packet transmission delay in the kth relay path. For the finite time-out at the destination, the maximum allowance A_m is adopted for receiving mth coded packet from all K paths, *i.e.,* $T_{m,k} \leq A_m$ for the mth coded packet reception in (1).

We generalize our algorithm to routing with imperfect scenario in (2). Since $\{\mathcal{Z}_{k,n}\}$ is selected for multiple K paths, it is reasonable to assume that the entire PTC codeword using the M time instants follow the same routes and avoid unnecessary re-routing. The imperfect route has failed path occurred when coded packets have no potential relay forwarding and does not reach destination, simply denoted as $\{\mathcal{Z}_{k,n=N_k}\} \neq \{\mathcal{D}\}$ for the kth failed path. Thus, the imperfect routes can be considered as erasure channels.

For expressing relations between relay locations and number of attempts, we define a function

$$f : (\{\mathcal{Z}_{k,n}\},\ \text{as } m\text{th coded packet propagation}) \rightarrow T_{m,k} \in \mathbb{N}, \tag{6}$$

and then interpret the generalized erasure indicator as

$$v_{m,k} = \begin{cases} 1, & T_{m,k} \leq A_m, \\ 0, & T_{m,k} > A_m. \end{cases} \tag{7}$$

Thus, given A_m, the end-to-end outage probability can be represented as

$$\begin{aligned}\mathbb{P}_{out} &= Pr\left(\mathbf{V}=\mathbf{0}_{K\times M}\middle|\ A_m\right)\\ &\geq Pr\left(\mathbf{V}=\mathbf{0}_{K\times M}\middle|\ A_m\to\infty\right)\\ &\overset{(a)}{=} Pr\left(\mathbf{v}_m=\mathbf{0}_{K\times 1}\middle|\ A_m\to\infty\right)\\ &= Pr\left(\{\mathcal{Z}_{k,n=N_k}\}\neq\{\mathcal{D}\},\ k=1,\ldots,K\right),\end{aligned} \tag{8}$$

where $A_m \to \infty$ denotes the sufficiently large allowance, and thus (a) shows the all-path-failed probability leads to the minimum value (when all K-path failed) as a lower bound.

For the generalized path gain $h_{m,k}$ corresponding to $\{\mathcal{Z}_{k,n}\}$ in (2), one can interpret the path gain as the product of link gains. This allows us to show that

$$\begin{aligned} h_{m,k} &= \prod_{n=1}^{N_k}\left[\sqrt{P_{SU}}\cdot g_{m,k,n}[t]\cdot|d(\mathcal{Z}_{k,n})|^{-\alpha/2}\right],\\ &s.t.\ \frac{P_{SU}|g_{m,k,n}[t]|^2|d(\mathcal{Z}_{k,n})|^{-\alpha}}{N_0+I_{PT}}\geq\beta,\ \text{from (4)},\end{aligned} \tag{9}$$

With the determined hop distance $d(\mathcal{Z}_{k,n})$, the mth coded data is stored in the buffer and then forwarded to the next hop as (4) satisfied. The generalized path gain in (9) is extended from product of Gaussian link gains [6] and is subjected to conditions with respect to per-hop SINR requirement.

We reinterpret virtual MIMO PTC end-to-end transmission in (2) connected to stochastic geometry. By substitution $v_{m,k}$ and $h_{m,k}$ with the above generalized erasure characteristics and path gain derived in (7) and (9), the bit error rate (BER) could be obtained from decoding (2) given A_m. With $A_m \to \infty$ in (8), one can find that

$$\text{BER} = P_e(1-\mathbb{P}_{out})+\frac{1}{2}\mathbb{P}_{out}\geq\frac{1}{2}\mathbb{P}_{out}, \tag{10}$$

where P_e denotes the error probability of "received" packets, and 1/2 indicates the error probability of blindly guessing the binary bit value $\{1, 0\}$ when the end-to-end outage occurs.

IV. Theoretical Analysis

In this section, we study the end-to-end outage probability and investigate the relation between per-hop transmit SNR and mean number of hops under different interference levels.

In multihop networking, the assumption of relays with equally spaced segments between $\mathcal{S}$–$\mathcal{D}$, *i.e.,* $d_s = d_{\mathcal{S}\text{–}\mathcal{D}}/\bar{N}$ with $\bar{N}$ hops, can simplify the analysis and provide a lower bound on the delivery delay [9]. Further followed multiple K paths with the same number of hops $\bar{N} = N_i$ for $i = 1,\ldots,K$ in [16], the theoretical end-to-end outage with K-path is denoted as $\mathbb{P}_{out}$ and could be represented as

$$\mathbb{P}_{out}\geq\left(1-p_s^{\bar{N}}\right)^K, \tag{11}$$

followed on the assumption of independent K-fold of the single-path end-to-end outage $\left(1-p_s^{\bar{N}}\right)$ with the i.i.d per-hop success probability p_s. From (4), p_s can be expressed as

$$\begin{aligned} p_s &= Pr\left\{\frac{P_{SU}G_{SU}d_s^{-\alpha}}{N_0+I_{PT}}\geq\beta\right\}\\ &= Pr\left\{G_{SU}\geq\frac{\beta}{P_{SU}d_s^{-\alpha}}(N_0+I_{PT})\right\}\\ &= \exp\left(-\frac{\beta N_0}{P_{SU}d_s^{-\alpha}}\right)\mathbb{E}\left[\exp\left(-\frac{\beta}{P_{SU}d_s^{-\alpha}}I_{PT}\right)\right]\\ &\overset{(a)}{=} \exp\left(-\frac{\beta N_0}{P_{SU}d_s^{-\alpha}}\right)\exp\left(-\lambda_{PT}d_s^2\left(\frac{\beta P_{PT}}{P_{SU}}\right)^{\frac{2}{\alpha}}\xi_\alpha\right),\\ &\overset{(b)}{=} \underbrace{\exp\left(-\frac{\beta N_0}{P_{SU}d_{\mathcal{S}\text{–}\mathcal{D}}^{-\alpha}}\bar{N}^{-\alpha}\right)}_{p_{s,nois}}\\ &\quad\cdot\underbrace{\exp\left(-\lambda_{PT}\left(\frac{d_{\mathcal{S}\text{–}\mathcal{D}}}{\bar{N}}\right)^2\left(\frac{\beta P_{PT}}{P_{SU}}\right)^{\frac{2}{\alpha}}\xi_\alpha\right)}_{p_{s,int.}}\\ &= p_{s,nois}\cdot p_{s,int.}\end{aligned} \tag{12}$$

where (a) comes from the moment generating function of I_{PT} [8], [10], $\xi_\alpha = \frac{2\pi^2}{\alpha\sin(\frac{2\pi}{\alpha})}$, and (b) is used with $d_s = d_{\mathcal{S}\text{–}\mathcal{D}}/\bar{N}$.

For the case of no interference, we combine (11) with $p_s = p_{s,nois}$ which comes from $\lambda_{PT} = 0$ in (12), and express the per-hop transmit SNR is bounded by

$$\frac{P_{SU}}{N_0}\leq\frac{\beta d_{\mathcal{S}\text{–}\mathcal{D}}^{\alpha}\bar{N}^{1-\alpha}}{-\ln\left(1-\mathbb{P}_{out}^{\frac{1}{K}}\right)}. \tag{13}$$

Under the interference-limited scenario and for the ease of exposition, we ignore the noise-effect and thus have $p_s = p_{s,int}$ in (12). Replacing p_s in (11) with $p_s = p_{s,int}$, we can show the per-hop transmit SNR is bounded by

$$\frac{P_{SU}}{N_0}\leq\left(\frac{\lambda_{PT}d_{\mathcal{S}\text{–}\mathcal{D}}^2\xi_\alpha}{-\bar{N}\ln\left(1-\mathbb{P}_{out}^{\frac{1}{K}}\right)}\right)^{\frac{\alpha}{2}}\left(\frac{\beta P_{PT}}{N_0}\right). \tag{14}$$

These theoretical approximations of transmit SNR under the scenarios with interference (14) and without (13) (as upper bounds) compare to the simulation results in Section V.

V. Simulation

In this section, we perform a multipath-search algorithm proposed in Section III for multipath routing in PPP network topology, and then apply the coding-aided scheme of PTC and repetition codes (REP) [17] verifying their validity for error control. Notice that our multipath cases with M data streams (coding-aided schemes either REP or PTC) follow the code rate $1/M$ for the same throughput comparison.

The system parameters, partly referred from [8], [16], are shown as follows: $\lambda_{SU1} = 5\times 10^{-4}$ or $\lambda_{SU2} = 10^{-3}$, $d_{\mathcal{S}\text{–}\mathcal{D}} = 200$, P_{SU} for transmit power (control), noise level $N_0 = 10^{-9}$ (*e.g.,* $P_{SU} = 0.1$ for $P_{SU}/N_0 = 80$ dB), λ_{PT} from 10^{-5} to 8×10^{-5}, $P_{PT} = 0.3$, $\alpha = 4$, and $\beta = 1$. With QPSK modulation and DFT-based PTC, BER performance is obtained from decoding in (2) using maximum a *posteriori* (MAP) criterion [6], [18] and with selected relays location

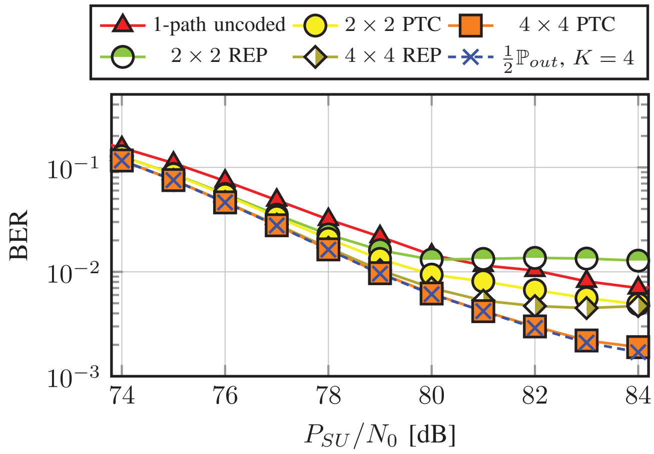

(a) No interference scenario: BER versus power control. The parameters are set as $\lambda_{SU1} = 5 \times 10^{-4}$, $d_{\mathcal{S}\text{-}\mathcal{D}} = 200$, $\alpha = 4$, and $\beta = 1$.

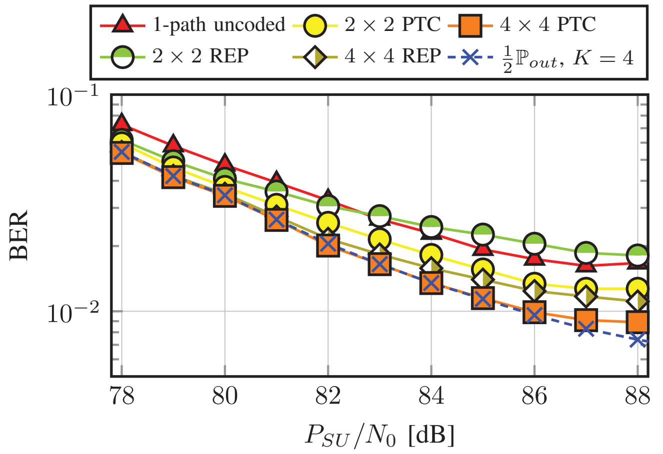

(b) With interference scenario: BER versus power control. The parameters are set as $\lambda_{SU2} = 10^{-3}$, $P_{PT} = 0.3$, $\lambda_{PT} = 10^{-5}$, $d_{\mathcal{S}\text{-}\mathcal{D}} = 200$, $\alpha = 4$, and $\beta = 1$.

Fig. 3. BER versus power control comparing different coding schemes followed with the proposed path-search algorithm. In the case (a) of no interference scenario and (b) with interference scenario. Single-path cases are uncoded (denoted as "uncoded") while multipath cases ($K = 2, 4$) are applied with the repetition code (REP) and the DFT-based PTC briefly denoted as "$M \times K$" REP and PTC on the figure. The 4×4 PTC outperforms REP in both scenarios (a) and (b) and almost reaches optimal values shown with $\frac{1}{2}\mathbb{P}_{out}$ obtained in (10). It demonstrates that PTC-aided multipath routing reaches decent error performance even under interference.

$\{\mathcal{Z}_{k,n}\}$ followed our proposed multipath-search algorithm. And thus coded packet reception (2) with generalized erasure indicators $v_{m,k}$ in (7) and path gains $h_{m,k}$ in (9) are also obtained and inherited from the selected relays $\{\mathcal{Z}_{k,n}\}$. The following three cases are discussed:

CASE I: Reliability and power control (in $A_m \to \infty$).

In Fig. 3 (a)–(b), we focus on error rate performance versus transmit SNR (power control) in the no interference case in Fig. 3 (a) and with the interference case in Fig. 3 (b). Here we consider the maximum allowance is sufficiently large, and compare uncoded, repetition coded, and path-time coded schemes. [1]

[1]For simplicity, we only focus on the interference impact from PUs to SUs. More interference interactions, *e.g.,* inter-interference from SUs to PUs, are investigated in [8].

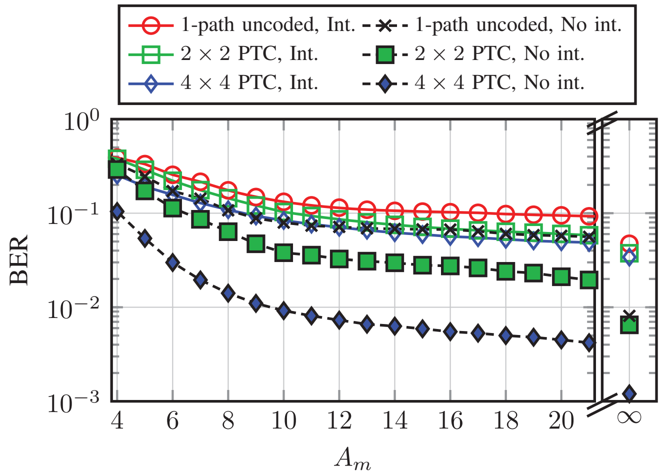

Fig. 4. BER versus allowance (A_m) comparison from single path (uncoded) to multipath (coded) under scenarios with interference and without. In the case of no interference cases (denoted "no int." on the figure), the parameters are set as $P_{SU} = 0.1$, $N_0 = 10^{-9}$, $\lambda_{SU2} = 10^{-3}$, $d_{\mathcal{S}\text{-}\mathcal{D}} = 200$, $\alpha = 4$, $\beta = 1$ (0 dB). In the case with interference (denoted "int." on the figure), the same parameters are followed and with interferers $P_{PT} = 0.3$, $\lambda_{PT} = 10^{-5}$. While single-path cases are uncoded with $K = 1$, multipath cases ($K = 2, 4$) are applied with DFT-based PTC briefly denoted as $M \times K$ REP and PTC on the figure. $A_m \to \infty$ shows sufficiently large (extreme) values for comparison finite allowances.

Followed our proposed multipath-search algorithm and (10), one-half of numerical end-to-end outage $\frac{1}{2}\mathbb{P}_{out}$ serves as the bench mark (lower bounded curve) for BER with coding-aided scheme. PTC with multipath outperforms uncoded and REP scenarios. It even validates that the 4×4 PTC reaches near optimal BER approaching $\frac{1}{2}\mathbb{P}_{out}$ in (10) with $P_e \to 0$. Thus, PTC-aided multipath routing using more paths, *e.g.* $K = 4$ here, provides robustness with error control under the scenario with interference and without.

CASE II: Reliability and allowance (in finite A_m).

Distinct to Fig. 3 (a)–(b) with the sufficiently large allowance $A_m \to \infty$, Fig. 4 depicts BER versus finite-range allowance A_m for the practical decoding scheme of receiving PTC packets y_m in (1). Fig. 4 provides an essential perspective for the practical system design criterion, *i.e.,* tradeoff relation between reliability (BER) and the maximum allowance. As the number of paths (multipath) K increases, the error rate decreases under the scenario with interference and without. This phenomenon manifests that multipath scheme propels low latency in end-to-end transmission especially greatly improved in no interference scenarios, *e.g.*, the lowest curve in Fig. 4.

CASE III: Relation among transmit power control, interference level, and the number of hops (in $A_m \to \infty$).

Fig. 5 (a) depicts SU power control in $\lambda_{SU2} = 10^{-3}$ versus different PU transmitter density (λ_{PT}). Both numerical and theoretical results are adopted with 4×4 PTC-aided multipath routing achieving BER $= \{5 \times 10^{-2},\ 2 \times 10^{-2}\}$, where lower BER can be viewed as higher quality of service (QoS) requirement. With adaptation of transmit power for fixed BER in Fig. 5 (a), the correspondent average number of hops can be observed in Fig. 5 (b). For the theoretical transmit power approximations, given the average number of hops, Fig. 5 (a) also shows the analytical results in (13) for the no interference

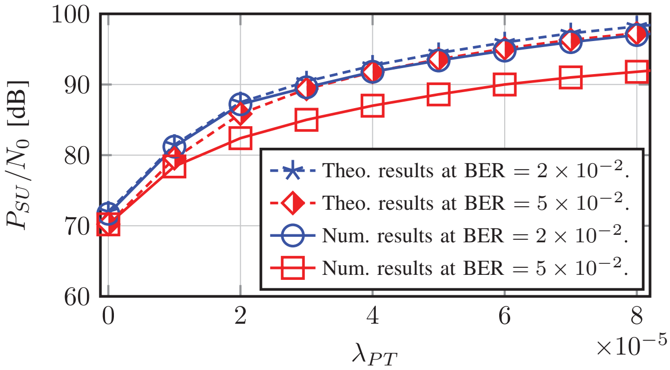

(a) Power control versus PU transmitter density (λ_{PT}).

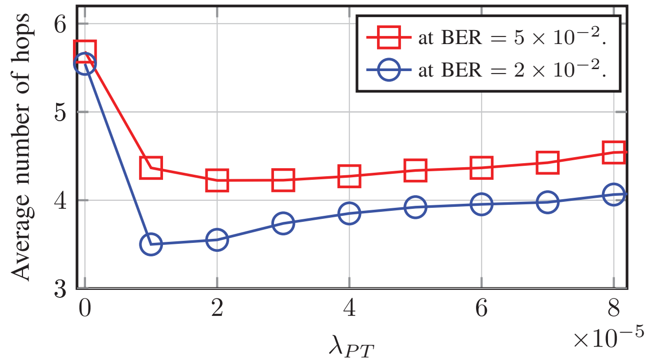

(b) Average number of hops versus PU transmitter density.

Fig. 5. The relation among power control, PU transmitter density (λ_{PT} for interference level), and average number of hops. The parameters are set as varying P_{SU}, $N_0 = 10^{-9}$ (*e.g.,* $P_{SU} = 0.1$ for $P_{SU}/N_0 = 80$ dB), $\lambda_{SU2} = 10^{-3}$, $P_{PT} = 0.3$, $d_{\mathcal{S}\text{-}\mathcal{D}} = 200$, $\alpha = 4$, and $\beta = 1$. In (a), numerical (Num.) and theoretical (Theo.) power control for fixed BER = $\{5 \times 10^{-2}, 2 \times 10^{-2}\}$ achieved by 4×4 PTC. Theoretic results of power control are obtained from (13) and (14). In (b), numerical average number of hops depends on transmit power control corresponding to numerical results in (a). With closely fitted results between theoretical and numerical in (a), the PTC-aided multipath routing demonstrates resilient operation with power control for the hop number and error control under interference scenarios.

($\lambda_{PT} = 0$) and (14) for the interference-limited scenarios λ_{PT} from 1×10^{-5} to 8×10^{-5}, where theoretical results are followed with BER $\simeq \frac{1}{2}\mathbb{P}_{out}$ achieved by 4×4 PTC in (10).

From observation in Fig. 5 (a), the theoretical and numerical results closely fit, especially in higher QoS requirement. These theoretical approximations of per-hop transmit power requirement in (13) and (14) provide insights to design power control under different interference levels for reliable and efficient PTC transmission.

VI. Conclusion

In this paper, we propose a multipath-search algorithm for multipath routing and coding-aided scheme with PTC for error-resilient control and efficient end-to-end transmission in CRAHNs. With only local information available, the proposed multipath-search algorithm provides near optimal routing policy to minimize the number of hops. By stochastic geometry analysis, we demonstrate that the resilient operation can be facilitated with the aid of path-time codes. The relations between reliability, power control, maximum allowance, and the number of hops are addressed. The analytical results for theoretical power control are also derived and closely fit the simulation results. These results provide insights to design power control under different interference levels for resilient operation in PTC transmission.

As many application scenarios in Internet of Things inevitably require spectrum sharing multi-hop networking, this research verifies a new avenue to facilitate resilient IoT networking design.

Acknowledgement

This study is conducted under the “Advanced communication technology research and laboratory development project” of the Institute for Information Industry which is subsidized by the Ministry of Economic Affairs of the Republic of China.

References

[1] H. Zhang, C. Jiang, R. Q. Hu, and Y. Qian, “Self-organization in disaster-resilient heterogeneous small cell networks,” *IEEE Network*, vol. 30, no. 2, pp. 116–121, 2016.

[2] K.-C. Chen and S.-Y. Lien, “Machine-to-machine communications: Technologies and challenges,” *Ad Hoc Networks*, vol. 18, pp. 3 – 23, 2014.

[3] S.-C. Hung, D. Liau, S.-Y. Lien, and K.-C. Chen, “Low latency communication for Internet of Things,” in *IEEE/CIC International Conference on Communications in China (ICCC)*, Nov. 2015, pp. 1–6.

[4] S.-Y. Lien, S.-C. Hung, and K.-C. Chen, “Optimal radio access for fully packet-switching 5G networks,” in *IEEE International Conference on Communications (ICC)*, Jun. 2015, pp. 3921–3926.

[5] I.-W. Lai, C.-H. Lee, and K.-C. Chen, “A virtual MIMO path-time code for cognitive ad hoc networks,” *IEEE Commun. Lett.*, vol. 17, no. 1, pp. 4–7, Jan. 2013.

[6] I.-W. Lai, C.-L. Chen, C.-H. Lee, K.-C. Chen, and E. Biglieri, “End-to-end virtual MIMO transmission in ad hoc cognitive radio networks,” *IEEE Trans. Wireless Commun.*, vol. 13, no. 1, pp. 330–341, Jan. 2014.

[7] A. Rabbachin, T. Quek, H. Shin, and M. Win, “Cognitive network interference,” *IEEE J. Sel. Areas Commun.*, vol. 29, no. 2, pp. 480–493, Feb. 2011.

[8] W.-C. Ao, S.-M. Cheng, and K.-C. Chen, “Phase transition diagram for underlay heterogeneous cognitive radio networks,” in *Proc. IEEE GLOBECOM*, Dec. 2010, pp. 1–6.

[9] J. G. Andrews, S. Weber, M. Kountouris, and M. Haenggi, “Random access transport capacity,” *IEEE Trans. Wireless Commun.*, vol. 9, no. 6, pp. 2101–2111, Jun. 2010.

[10] F. Baccelli, B. Blaszczyszyn, and P. Mühlethaler, “An Aloha protocol for multihop mobile wireless networks,” *IEEE Trans. Inf. Theory*, vol. 52, no. 2, pp. 421–436, Feb. 2006.

[11] Y. Chen and J. G. Andrews, “An upper bound on multihop transmission capacity with dynamic routing selection,” *IEEE Trans. Inf. Theory*, vol. 58, no. 6, pp. 3751–3765, Jun. 2012.

[12] K. Stamatiou and M. Haenggi, “Delay characterization of multihop transmission in a Poisson field of interference,” *IEEE/ACM Transactions on Networking (TON)*, vol. 22, no. 6, pp. 1794–1807, 2014.

[13] M. Marina and S. Das, “On-demand multipath distance vector routing in ad hoc networks,” in *Proc. IEEE ICNP*, Nov. 2001, pp. 14–23.

[14] P. Djukic and S. Valaee, “Reliable packet transmissions in multipath routed wireless networks,” *IEEE Trans. Mobile Comput.*, vol. 5, no. 5, pp. 548–559, May 2006.

[15] S. Fashandi, S. Gharan, and A. Khandani, “Path diversity over packet switched networks: Performance analysis and rate allocation,” *IEEE/ACM Trans. Netw.*, vol. 18, no. 5, pp. 1373–1386, Oct. 2010.

[16] P.-Y. Chen, S.-M. Cheng, W.-C. Ao, and K.-C. Chen, “Multi-path routing with end-to-end statistical QoS provisioning in underlay cognitive radio networks,” in *Proc. IEEE INFOCOM WKSHPS*, Apr. 2011, pp. 7–12.

[17] W. C. Huffman and V. Pless, *Fundamentals of error-correcting codes*. Cambridge university press, 2010.

[18] Y.-C. Chen, I.-W. Lai, K.-C. Chen, W.-T. Chen, and C.-H. Lee, “Transmission latency and reliability trade-off in path-time coded cognitive radio ad hoc networks,” in *Proc IEEE GLOBECOM*, Dec. 2014, pp. 1084–1089.